Ⓔ

COLOR GRADIENTS DETECTED IN THE HD 15115 CIRCUMSTELLAR DISK

John H. Debes,[1] Alycia J. Weinberger,[1] and Inseok Song[2]

ABSTRACT

We report *HST* NICMOS coronagraphic images of the HD 15115 circumstellar disk at 1.1 μm. We find a similar morphology to that seen in the visible and at *H* band—an edge-on disk that is asymmetric in surface brightness. Several aspects of the 1.1 μm data are different, highlighting the need for multiwavelength images of each circumstellar disk. We find a flattening to the western surface brightness profile at 1.1 μm interior to $2''$ (90 AU) and a warp in the western half of the disk. We measure the surface brightness profiles of the two disk lobes and create a measure of the dust scattering efficiency between 0.55 and 1.65 μm at $1''$, $2''$, and $3''$. At $2''$ the western lobe has a neutral spectrum up to 1.1 μm and a strong absorption or blue spectrum >1.1 μm, while a blue trend is seen in the eastern lobe. At $1''$ the disk has a red F110W $-$ *H* color in both lobes.

Subject headings: circumstellar matter — stars: individual (HD 15115)

Online material: color figures

1. INTRODUCTION

Raw material from the interstellar medium is processed through circumstellar disks into many different types of planetary bodies. Debris disks are a useful environment to study the composition of planetesimals that form around stars different from our own Sun. Multiwavelength scattered light observations of disks provide one avenue for determining the composition of dust caused by collisions of planetesimals.

HD 15115 possesses one of a growing number of spatially resolved debris disks amenable to multiwavelength observations. HD 15115 is an F2 star at a distance of 45 $\pm$ 1 pc (van Leeuwen 2007) and was observed to have an IR excess (Silverstone 2000). Unresolved emission from its disk was detected at 60, 100, and 850 μm, implying a ring at $\sim$35 AU with a temperature of 62 K (Zuckerman & Song 2004; Decin et al. 2003; Williams & Andrews 2006). Recently, Kalas et al. (2007, hereafter KFG07) discovered circumstellar emission from a combination of *Hubble Space Telescope* Advanced Camera for Surveys (*HST* ACS) and Keck near-IR AO coronagraphic imaging. Surface brightness (SB) profiles were reported for *V* and *H* bands. Furthermore, they observed an extreme size and brightness difference between the two lobes of the disk and shape asymmetries around the disk midplane similar to that seen around β Pictoris and indicative of a second disk at a different inclination (Kalas & Jewitt 1995; Golimowski et al. 2006). We have imaged HD 15115 at 1.1 μm with *HST*; we present our observations in § 2 and analyze the results in § 3. We discuss the implications of our work in § 4.

2. OBSERVATIONS

We observed HD 15115 with the *Hubble Space Telescope*'s Near-Infrared and Multi-Object Spectrometer (NICMOS) (Thompson et al. 1998) using the coronagraph in Camera 2. We used the F110W filter with a central wavelength of 1.1 μm (0.8–1.4 μm). Observations were taken on 2006 October 20 for HD 15115 and HD 16647, the PSF reference.

Accurate disk photometry requires a correct scaling ratio between the target star and its PSF reference. Both stars would saturate the detector in the shortest exposure. Therefore, we estimated the F110W flux density for both stars with synthetic photometry using the CALCPHOT task of the SYNPHOT[3] package in conjunction with Kurucz models tabulated in the SYNPHOT library. We found a best-fit match to HD 15115's luminosity and effective temperature based on its parallax from the *Hipparcos* satellite, its Tycho-2 *B* and *V* photometry, and 2MASS *J*, *H*, and K_s photometry. The model assumed a solar metallicity, and the best fit was for a log g = 5.0, $T_{\rm eff}$ = 6750 K star, with a luminosity of 3.11 $L_\odot$. We fit solar metallicity models to HD 16647, finding a best fit for a log g = 5.0, $T_{\rm eff}$ = 6750 K star and a luminosity of 4.01 $L_\odot$. The resulting SYNPHOT scaling in F110W is 0.600. Based on previous experience (Debes et al. 2008 for example), SYNPHOT is accurate to $\sim$3%, which we will adopt as our a priori estimate of the scaling uncertainty. Coronagraphic images of the disk were taken at two spacecraft orientations. The images were subtracted, registered, and combined following the procedures of Debes et al. (2008). The individual subtracted and combined images are shown in Figure 1.

3. ANALYSIS

Figure 1 shows that the disk is detected at the same position angle (PA) as KFG07, despite the presence of one strong residual streak close to the position of the eastern lobe of the disk (feature A in Fig. 1). Perpendicular to the disk, strong residuals also exist. We measured the PA, full width at half-maximum (FWHM) of the disk midplane, and SB profiles as a function of radius from the central star.

3.1. *Disk Geometry*

We measured the PA and FWHM of the western lobe of the disk from $0.68''$ (30 AU) to $3.69''$ (165 AU). For the eastern lobe we took measurements from $0.68''$ to $3.0''$ (135 AU). In our analysis we rotated the final disk images so that the disk midplane was oriented along an image row. We took 3×13 ($0.23'' \times 0.98''$) pixel cuts of the disk centered on the brightest pixel of the disk and summed in a direction perpendicular to the midplane direction. We then fit a Gaussian curve to the

[1] Department of Terrestrial Magnetism, Carnegie Institution of Washington, Washington, DC 20015; debes@dtm.ciw.edu.

[2] Department of Physics and Astronomy, University of Georgia, Athens, GA 30605.

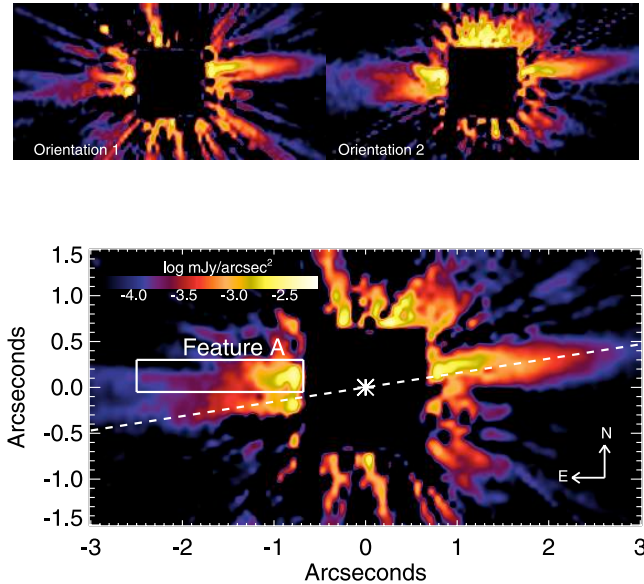[3] See http://www.stsci.edu/resources/software_hardware/stsdas.

FIG. 1.—*Top*: False-color images of the observations of HD 15115 in the F110W filter at two spacecraft orientations. The images are logarithmically scaled. *Bottom*: False-color, final combined image of the HD 15115 disk, showing the contaminating feature A. The dashed line represents the nominal position angle of the disk at 278.9°, while the asterisk represents the position of the star. We have masked out separations in the disk within 0.68″, where PSF subtraction residuals dominate. Noticeable are a warp on the western lobe, and the asymmetries between the western and eastern lobes.
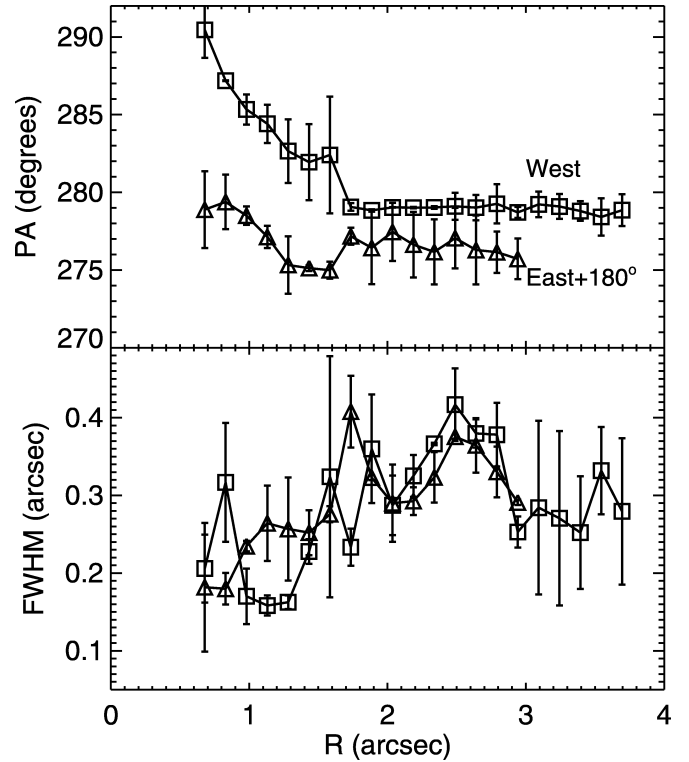

FIG. 2.—Measurements of the HD 15115 disk midplane PA (*top*) and FWHM (*bottom*) as a function of distance for the two lobes of the disk. Squares represent the western lobe, while triangles represent the eastern lobe. The sharp rise in PA for the western lobe interior 1.7″ is due to the warp, and the eastern lobe's PA beyond 1.8″ is marginally different than the western lobe. [*See the electronic edition of the Journal for a color version of this figure.*]

disk emission to measure the location of the midplane (and thus the local PA) as well as the FWHM of the disk. We took an average of the values for both orientations and estimated the uncertainty as being half the difference between the two measurements. Figure 2 shows the PA and FWHM of the western lobe of the disk as a function of radius. Beyond 1.7″, we find a PA for the disk of 278.9° ± 0.2°, which is consistent with KFG07's value of 278.5° ± 0.5°. However, interior to 1.7″, we note that the disk PA increases with decreasing distance from the star to a maximum PA of 290° ± 1° at 0.68″. The changing PA of the midplane is seen at both orientations. Furthermore, we find at 2″ a FWHM of 0.29″ ± 0.04″ which is consistent with the FWHM of 0.19″ ± 0.1″ reported by KFG07. The median FWHM of the disk from 0.68″ to 3.69″ is 0.26″ ± 0.07″. The FWHM at 1.1 μm is broadened by the NICMOS F110W PSF, which has a FWHM of 0.1″, implying an intrinsic FWHM for the disk midplane of ~0.24″ or 11 AU.

Measurement of the eastern side of the disk is complicated by the contamination of feature A from PSF subtraction. To measure the FWHM and PA, we masked out pixels heavily contaminated by this feature. We again took the average of the two sets of measurements and estimated the uncertainties as being half the difference between the two measurements. We find no evidence of a warp in the eastern lobe, which has a median PA of 96.6° ± 1.3°. To compare to the PA of the western side we add 180° to get 276.6°, consistent with no significant bowing in the large-scale structure of the disk as is seen for HD 61005 (Hines et al. 2007). The median value of the eastern FWHM is 0.29″ ± 0.06″.

3.2. *Surface Brightness Profiles*

Figure 3 shows a comparison of the 1.1 μm SB profiles in Δm_{F110W} arcsec^{-2} relative to the central star (m_{F110W} = 6.12) for the eastern and western lobes of the disk by taking 0.23″

× 0.23″ apertures centered on the midplane of the disk. Between 0.7″ and 1.8″, the disk SB of the western lobe falls as $r^{-1.4\pm0.1}$, while at radii >1.8″, the SB drops as $r^{-3.56\pm0.06}$. The eastern lobe drops steadily as $r^{-2.14\pm0.06}$ from 0.7″ to 3″.

3.3. *Scattering Efficiency vs. Wavelength*

Combining our data with the reported *V* and *H* SB data, a measure of the scattering efficiency of the dust around HD 15115 can be constructed. The measured SB at any radius in the disk can be self-consistently modeled for composition and grain size distribution provided a knowledge of the density distribution of the dust is known (see details in Debes et al. 2008). The SB of a dust disk at a particular radius is $\propto F_\star \phi(\theta) Q_{sca}(L_\star/L_{IR})$, where $\phi(\theta)$ is the phase function of the dust at a particular scattering angle, Q_{sca} is the scattering efficiency of the dust, and $L_\star/L_{IR}$ is the ratio of stellar luminosity to the IR luminosity of the dust distribution. This is difficult for HD 15115 because the density distribution of the dust is not known through, for example, spatially resolved thermal emission images. However, multiwavelength imaging can provide useful compositional information even in the absence of spatially resolved thermal emission constraints. In the case of HD 15115, three images at different wavelengths will be insufficient to provide a definitive picture, but can constrain certain compositions.

In order to compare results across different wavelengths, instruments, and telescopes, it is imperative that a careful and consistent treatment of SB measurements is implemented. Observations of disks at different wavelengths can be affected by the respective PSFs of telescopes with different diffraction lim-
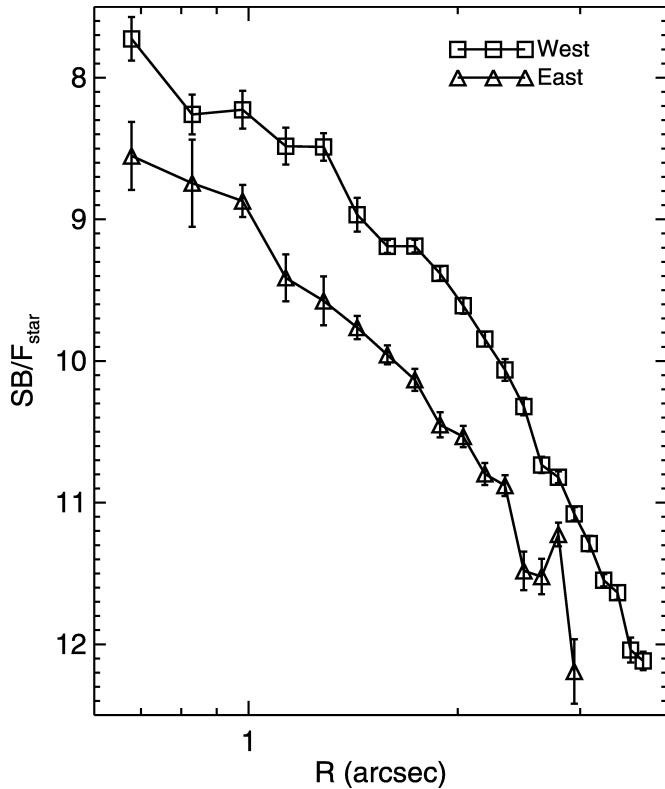
FIG. 3.—Surface brightness profiles of the eastern and western lobes of the disk in F110W magnitudes per square arcsecond for a 0.23″ × 0.23″ aperture. No corrections were applied. The symbols are the same as in Fig. 2. [*See the electronic edition of the Journal for a color version of this figure.*]

FIG. 4.—Comparison of the scattering efficiency (or color) vs. wavelength of HD 15115's disk at 1″ (45 AU), 2″ (90 AU), and 3″ (135 AU). The symbols are the same as in Fig. 2. The disk dramatically changes color over wavelength and distance from the central star. [*See the electronic edition of the Journal for a color version of this figure.*]

its and Strehl ratios, but no standard technique is applied to the study of circumstellar disks. Intuitively, one would expect minor corrections as a function of wavelength provided that the disk structure did not significantly change between wavelengths and that the disk itself was mostly resolved. KFG07 estimated aperture corrections using point source PSFs. Other methods have included deconvolution of the data (Golimowski et al. 2006), or using apertures that capture the majority of the observed emission from the disk at each wavelength (Schneider et al. 1999; Weinberger et al. 2002; Debes et al. 2008). We modeled the effect of the different PSFs of NICMOS, ACS, and Keck *H*-band adaptive optics on the measured surface brightness for the 0.23″ × 0.23″ aperture.

Our approach to calculating the corrections derives from the reliable theoretical PSFs generated by Tiny Tim[4] for *HST* as well as using a Keck *H* PSF corresponding to the October observations of HD 15115 (M. Fitzgerald 2008, private communication). We took the PSFs for each instrument and convolved them with model disks constructed from the measured power-law slopes and disk FWHMs for each observation. We then measured the SB as a function of distance for the original and convolved models with the 0.23″ × 0.23″ aperture in F110W and a 0.25″ × 0.25″ aperture for *V* and *H* and took the ratio as a single-valued multiplicative correction to the observed SB profiles. We verified that the slope of the surface brightness profiles did not change due to convolution. To estimate the uncertainty in this correction, we used the standard deviation of the measurements between 2″ and 3″, the region where all the observations overlap. For the ACS coronagraphic
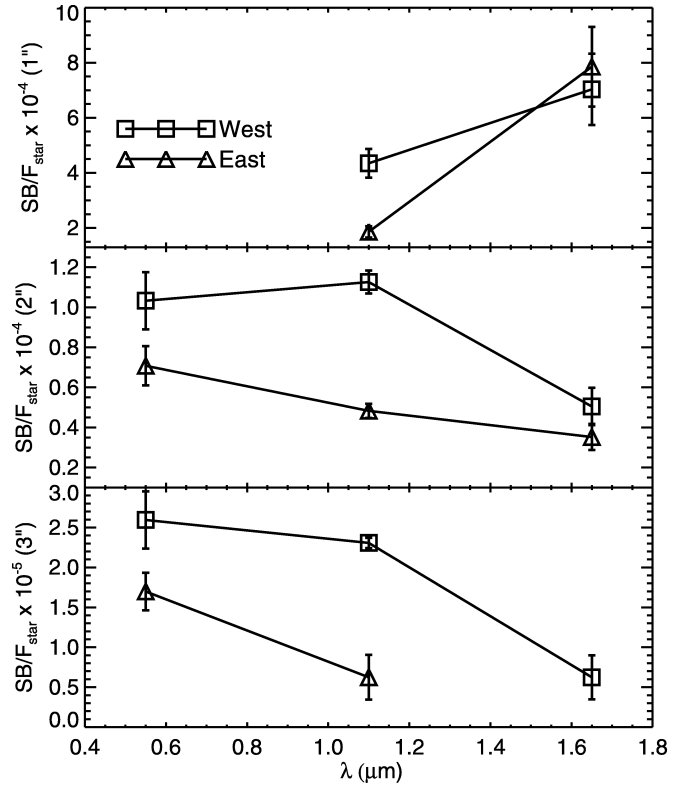
PSF, we found a correction of 1.23 ± 0.02, for the *H* band we found a correction of 1.56 ± 0.06, and for F110W we found a correction of 1.36 ± 0.04.

To compare the NICMOS and other measurements, we must make a correction for the slightly different photometric aperture sizes of 0.23″ × 0.23″ and 0.25″ × 0.25″, respectively. To do this we oversampled our model NICMOS images by a factor of 3 and calculated the predicted difference in SB measurements between our 0.23″ × 0.23″ aperture and a 0.25″ × 0.25″ one. This multiplicative correction changes with distance from the star, and ranges from 1.2 to 0.8.

In Figure 4 we plot SB/$F_{\nu,\star}$ as a function of wavelength for HD 15115's two disk lobes at 1″, 2″, and 3″. This observed quantity is ∝Q_{sca}. Our 1.1 μm data provide a third point in the measure of HD 15115's scattering efficiency when combined with the 0.55 μm (*V*) and 1.65 μm (*H*) measurements in KFG07. We derive the uncertainties in the scattering efficiency for 0.55 and 1.65 μm based on Figure 3 in KFG07. Where no error bars were given for the 1.65 μm data in KFG07, we assumed an uncertainty of 20%. In the western lobe at 2″, we find that the disk's scattering efficiency is neutral out to 1.1 μm but then drops such that the spectrum is blue at 1.65 μm. The spectrum is the same from 0.55 to 1.65 μm at 3″. At 2″, the eastern lobe is strongly blue and at 3″ the blue trend continues out to 1.1 μm. KFG07 did not report SB for the *H* data at 3″, but if the spectrum is the same as the inner part of the disk, one would expect the blue trend to continue to longer wavelengths.

Finally, interior to about 1.8″, we can get a rough sense of the near-IR colors of the disk in the east and west. We took KFG07's measurements of the two lobes in *H* at 1″ and com-

pared them to our data. In both cases the disk is red, the result of the difference in SB profiles between F110W and H interior to 2″.

4. DISCUSSION

The new features we have observed in the disk at 1.1 μm add questions to the nature of the disk and the dust. The increase in PA toward the inner part of the disk could be caused by a genuine warp, or perhaps the presence of a second disk inclined at >12° from the main disk as is seen in β Pictoris. This is supported by the detection of an asymmetry in the northern part of the disk seen in the ACS and H data of KFG07.

KFG07 noted an overall blue $V - H$ color for the western lobe of the disk. The presence of a neutral scattering efficiency out to 1.1 μm as well as a red F110W $- H$ color interior to 2″ suggests that the spectrum of the HD 15115 disk is more complicated than the V and H data suggest. The abrupt change in scattering efficiency beyond 2″ from F110W to H may be due to the presence of strong absorption at ~1.65 μm. One candidate would be strong absorption due to water ice, something not yet detected in the scattered light of a disk. If that is the case, even deeper absorption should be present at 2 and 3.5 μm. Two possibilities exist to explain the red F110W $- H$ color of the inner disk—either there is evidence of strong absorption due to olivine (which has an absorption feature at 1 μm), or the presence of a very red material in the disk, possibly similar to what is seen in HD 100546 (Ardila et al. 2007) or HR 4796A (Debes et al. 2008).

The age of HD 15115 is not well constrained, which would be helpful in understanding the origins of the debris disk. Kinematically, it is marginally consistent with membership in the 12 Myr old β Pictoris moving group (BPMG) (Moór et al. 2006). However, this is not borne out by backtracking the position of HD 15115 based on its proper motion and radial velocity using the methods of Ortega et al. (2002) and Song et al. (2003) nor is kinematics a reliable selector of a moving group (Song et al. 2002). Most other indicators point to a >100 Myr age. Nordström et al. (2004) determined an age of 900 Myr, but this age is uncertain given their methodology—the lower limit for the age is 0, while the upper limit is 2.2 Gyr. Ca II H and K line indicators point to an age of 500 Myr (Silverstone 2000). Although not an accurate age indicator for early F-type stars, the lithium 6708 Å feature shows an equivalent width of 40 mÅ (I. Song 2008, in preparation), which is consistent with ~100 Myr Pleiades stars. As a comparison, previously recognized 30 Myr old (Tucana–Hor A) stars or younger early F-type stars all show equivalent widths for Li

of ~100 mÅ. The evidence to date points to an older age for HD 15115.

HD 15115 is a prime example of the potential complexity of nearby circumstellar debris disks. It possesses a strange brightness asymmetry in its outer reaches that extends into about 2″ (90 AU). This asymmetry, however, is a function of wavelength, and at least part of the cause may be compositional or grain population differences between the two sides of the disk. KFG07 investigated whether the close passage of a star might explain the strange morphology of the disk. They found a candidate object, HIP 12545, that might have passed very close to the debris disk of HD 15115, but while its motion is consistent with being a comoving object, backtracking of the two stars' positions back in time based on their *Hipparcos*/ Tycho-2 astrometry and radial velocities shows that they are more widely separated in the past than they are now and could not have interacted.

The fact that we measure a warp only in the western part of the disk around 1″ suggests that HD 15115 has an even more complex structure. It would be useful to confirm the presence of this structure in the disk at other wavelengths. This is not easily done in the visible, unless STIS is refurbished in the next servicing mission—it is the only instrument able to image to within ~1″ in the visible. Follow-up H and K (or F160W or F205W images with *HST*) will be useful to look for the warp as well as constrain the ultimate nature of the composition of the grains in the disk. If water ice is indeed present, it will show strong absorption at around 2 and 3.5 μm. Therefore, K and L band images of the scattered light disk are crucial.

What are the other possibilities to explain both the warp, the asymmetry, and the varying nature of the dust grains? One possibility is that the asymmetry is caused by a relatively recent collision that has injected many particles recently into the disk. Such an event is rare given the collisional times of the parent bodies and the timescale for such an event to be evenly spread in azimuth. Similar asymmetries have been seen in the mid-IR with β Pictoris (Weinberger et al. 2003), and it is striking that HD 15115 shares many of traits with this well-known disk.

REFERENCES

Ardila, D. R., Golimowski, D. A., Krist, J. E., Clampin, M., Ford, H. C., & Illingworth, G. D. 2007, ApJ, 665, 512
Debes, J. H., Weinberger, A. J., & Schneider, G. 2008, ApJ, 673, L191
Decin, G., Dominik, C., Waters, L. B. F. M., & Waelkens, C. 2003, ApJ, 598, 636
Golimowski, D. A., et al. 2006, AJ, 131, 3109
Hines, D. C., et al. 2007, ApJ, 671, L165
Kalas, P., Fitzgerald, M. P., & Graham, J. R. 2007, ApJ, 661, L85 (KFG07)
Kalas, P., & Jewitt, D. 1995, AJ, 110, 794
Moór, A., Ábrahám, P., Derekas, A., Kiss, C., Kiss, L. L., Apai, D., Grady, C., & Henning, T. 2006, ApJ, 644, 525
Nordström, B., et al. 2004, A&A, 418, 989

Ortega, V. G., de la Reza, R., Jilinski, E., & Bazzanella, B. 2002, ApJ, 575, L75
Schneider, G., et al. 1999, ApJ, 513, L127
Silverstone, M. D. 2000, Ph.D. thesis, UCLA
Song, I., Bessell, M. S., & Zuckerman, B. 2002, A&A, 385, 862
Song, I., Zuckerman, B., & Bessell, M. S. 2003, ApJ, 599, 342
Thompson, R. I., Rieke, M., Schneider, G., Hines, D. C., & Corbin, M. R. 1998, ApJ, 492, L95
van Leeuwen, F. 2007, A&A, 474, 653
Weinberger, A. J., Becklin, E. E., & Zuckerman, B. 2003, ApJ, 584, L33
Weinberger, A. J., et al. 2002, ApJ, 566, 409
Williams, J. P., & Andrews, S. M. 2006, ApJ, 653, 1480
Zuckerman, B., & Song, I. 2004, ApJ, 603, 738